Chinese Chemical Letters 36 (2025) 110252

Contents lists available at ScienceDirect

Chinese Chemical Letters

journal homepage: www.elsevier.com/locate/cclet

Discovery and enantioselective total synthesis of antitumor agent asperfilasin A *via* a regio- and diastereoselective Nazarov cyclization

Fengqing Wang[a,1], Changxing Qi[a,1], Chunmei Chen[a,1], Qin Li[a], Qingyi Tong[a], Weiguang Sun[a], Zhengxi Hu[a], Minyan Wang[b,*], Hucheng Zhu[a,*], Lianghu Gu[a,*], Yonghui Zhang[a,*]

[a] *Hubei Key Laboratory of Natural Medicinal Chemistry and Resource Evaluation, Tongji Medical College, Huazhong University of Science and Technology, Wuhan 430030, China*

[b] *State Key Laboratory of Coordination Chemistry, School of Chemistry and Chemical Engineering, Nanjing University, Nanjing 210093, China*

ARTICLE INFO

Article history:
Received 15 May 2024
Revised 9 July 2024
Accepted 15 July 2024
Available online 15 July 2024

Keywords:
Cytochalasan
Antitumor activity
Nazarov cyclization
Basic nitrogen
Contiguous stereocenters
DFT calculations

ABSTRACT

Asperfilasin A (**1**), featuring a unique 5/5 cyclopenta[*c*]pyrrol-one bicyclic core, represents a newly discovered skeletal cytochalasan isolated from *Aspergillus flavipes*. The enantioselective total synthesis was efficiently accomplished from the key intermediate (*S*)-**6** with three contiguous stereocenters in 5 steps and the synthetic **1** induced G2/M-phase cell cycle arrest of HT29 cells and apoptosis of HL60 and NB4 cells by activation of caspase-3 and degradation of PARP. (*S*)-**6**, bearing three contiguous chiral centers, was efficiently constructed by a novel Nazarov cyclization reaction containing basic nitrogen, which was less developed, primarily due to the incompatibility of basic nitrogen under acidic reaction conditions. This reaction allows a wide range of pentadienone substrates containing basic nitrogen to undergo Nazarov cyclization in a single regioselective and diastereoselective manner and is capable of generating three stereocenters simultaneously. Furthermore, the mechanism of the Nazarov cyclization and the origin of the regio- and diastereoselectivity were elucidated by DFT calculations and deuteration experiments, providing valuable insights into the reaction and serving as a guide for future applications involving substrates containing basic nitrogen.

Cytochalasans are a large group (>500 members) of fungal-derived natural products [1,2], exhibiting a wide range of biological properties such as cytotoxic [3,4], phytotoxic [5–8], antimicrobial [9,10] and antiparasitic activities [11,12]. A large number of cytochalasans were isolated by our group and coworkers [13], such as asperchalasines A-D [14], epicochalasines A, B [15], and asperflavipines A, B [16]. So far, cytochalasans have attracted considerable attention in the fields of synthesis [17–23], biosynthesis [24–28], and pharmacology [29–31] because of their biological diversity and remarkable structure. Structurally, almost all cytochalasans comprise one common unit, an isoindolone moiety bearing a 5/6 ring system, and their general synthetic strategy for the isoindolone core often started from the construction of 5-membered lactam followed by Diels-Alder cyclization [17–23]. However, the synthesis of the newly discovered cytochalasan asperfilasin A (**1**), featuring a unique 5/5 cyclopenta[*c*]pyrrol-one bicyclic core, necessitated the development of innovative synthetic methodology.

Nazarov cyclization is recognized as a highly efficient tool to generate diverse cyclopentenone motifs, known as a 4π conrotatory electrocyclization of divinyl ketones to cyclopentenones in one step [32,33]. Despite the advancements in this field [34–37], the exploration of aliphatic chain γ-aza-substituted pentadienones has not been reported. This is primarily due to the incompatibility of the basic nitrogen in acidic reaction conditions. Additionally, the incorporation of auxiliary groups to govern chirality in Nazarov cyclization reactions has also been scarce. Flynn achieved the asymmetric synthesis of cyclopentenones using oxazolidinone auxiliaries. However, the diastereoselectivity was not well controlled [38] until the auxiliaries were directly linked to the α-position of carbonyl [39–41], and the mechanism of oxazolidinone-based stereocontrol is driven by allylic strain *via* computational studies [42]. Nazarov cyclization controlled by chiral sulfoxide was also proved to be poor (Scheme 1a) [43]. Therefore, the development of divinyl ketones containing basic nitrogen with side-chain-controlled chirality remains a challenging area for Nazarov cyclization.

* Corresponding authors.
E-mail addresses: wangmy@nju.edu.cn (M. Wang), zhuhucheng@hust.edu.cn (H. Zhu), gulianghu@hust.edu.cn (L. Gu), zhangyh@mails.tjmu.edu.cn (Y. Zhang).
[1] These authors contributed equally to this work.

https://doi.org/10.1016/j.cclet.2024.110252
1001-8417/

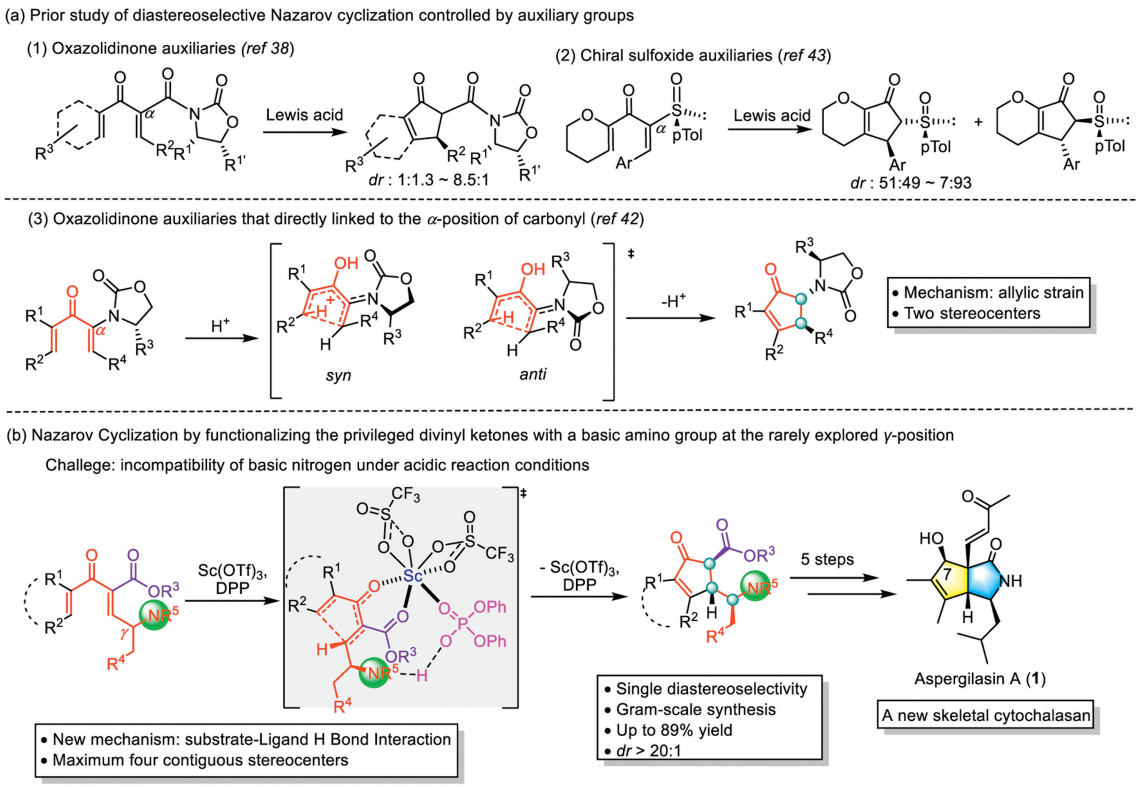

Scheme 1. Asperfilasin A and diastereoselective Nazarov cyclization controlled by auxiliary groups.

Herein, asperfilasin A (**1**) was isolated and characterized as the first example of cytochalasan with 5/5 cyclopenta[*c*]pyrrol-one bicyclic core from *Aspergillus flavipes*. The synthetic endeavor employing a novel Nazarov cyclization not only confirmed the structure of **1** but also yielded ample quantities of samples for subsequent biological investigations. Asperfilasin A exhibited good antitumor activity. Moreover, we delineated a new Nazarov cyclization containing basic nitrogen with stereospecific diastereoselectivity that four contiguous stereocenters can be simultaneously formed, including one outside the ring of the pentadienone (Scheme 1b). The substrate scope was investigated and the mechanism of this reaction was also elucidated by DFT calculations and deuterated experiments.

Based on the NMR data, the planar structure of **1** was elucidated (see Supporting information for details). However, there was no diagnostic signal for H-7 to determine its configuration. Therefore, the ^{13}C NMR calculations with the DP4+ probability analysis for both epimers (**1** and **2**) of C-7 were conducted. The results showed that 7*R* was the real relative configuration of **1** with 100% probability. To determine the absolute configuration of **1**, quantum chemical ECD calculations were employed. The theoretically calculated ECD spectrum of **1** was in good agreement with the experimental ECD spectrum (Fig. S5 in Supporting information), thus confirming the absolute structure of **1** to be 3*S*,4*R*,7*R*,8*R*. Although the structure and configuration of asperfilasin A can be determined through the above methodologies, there may still be some uncertainty. Therefore, synthetic methods are essential to fully determine the configuration and subsequent pharmacological investigations.

The discovery of asperfilasin A (**1**) featuring an unprecedented scaffold led us to investigate its plausible biosynthetic pathway. The basic skeletons of cytochalasans were confirmed to be generated *via* PKS-NRPS hybrid pathways, involving Knoevenagel condensation and Diels-Alder cycloaddition as key steps to construct the tricyclic ring systems (Scheme 2) [24,44]. The biosynthetic pathway of **1** was proposed to start from the original precursor aspochalasin P (**3**), which was isolated both in our previous and present studies. For **1**, aspochalasin P underwent a series of oxidative and reductive reactions to form the intermediate **iv**, which further provided the key intermediate **v** with a cyclopropane moiety. Subsequently, the unexpected 5/5 fused skeleton of **vi** was constructed *via* oxidative cleavage of the C-7 – C-8 bond and dehydration of the hydroxyl group at C-6. Finally, **1** was generated by an additional oxidative cleavage of the C-14–C-15 bond to lose the fragment of C-15–C-21 from **vii**.

Fascinated by the unique structural backbone of asperfilasin A, the total synthesis of **1** was further investigated. Initially, the previously established synthetic strategy of cytochalasans was attempted to follow wherein the chiral five-membered lactam ring was synthesized first, followed by the synthesis of another ring. Regrettably, with our hands, these approaches proved ineffective (see Supporting information for details). It is speculated that the 5/6 ring formation is feasible, while the synthesis of the 5/5 ring encountered challenges, possibly attributed to heightened ring strain. Instead, the cyclopentenone ring was synthesized first to complete the total synthesis of **1** and the Nazarov cyclization was the pivotal step in the overall synthesis.

We started our synthesis as depicted in Scheme 3. Alkynoate **4** (detailed synthetic procedures see Supporting information) was utilized in a one-pot, palladium-mediated *syn*-hydrostannylation, followed by a copper-mediated Stille-Scott cross-coupling with tigloyl chloride, directly affording defined stereochemically divinyl ketones (*S*)–**5** [38,45]. Although this method had been previously reported, it was the first application of an alkynoate substrate containing basic nitrogen. With an ample supply of (*S*)–**5** in hand, our initial attempts utilizing $SnCl_4$ yielded the anticipated cyclopentenones (*S*)–**6** as a single entity in 25% yield. Further investigation of Lewis acids was undertaken to determine the optimal synthesis condition (Table 1).

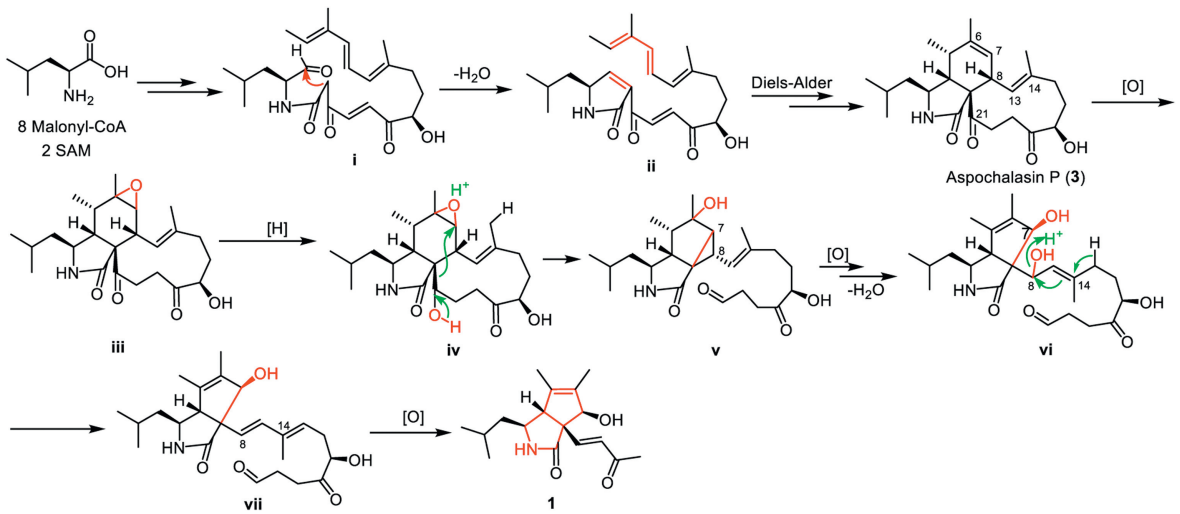

Scheme 2. Plausible biogenetic pathway of **1**.

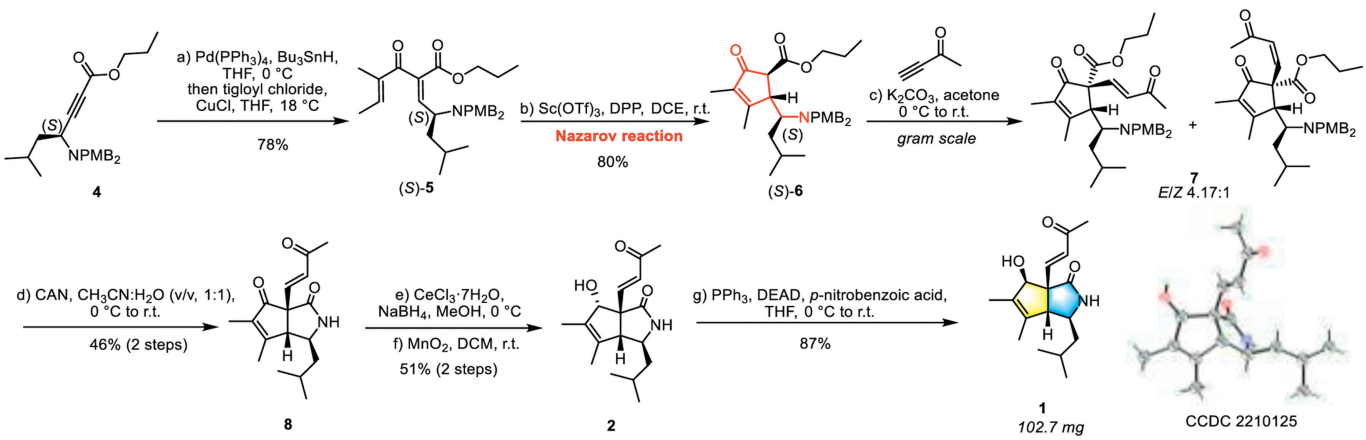

Scheme 3. Total synthesis of **1**. PMB = *p*-methoxybenzyl, CAN = ammonium ceric nitrate, DEAD = diethyl azodiformate.

Table 1
Selected conditions for the Nazarov cyclization of (*S*)–**5**.[a]

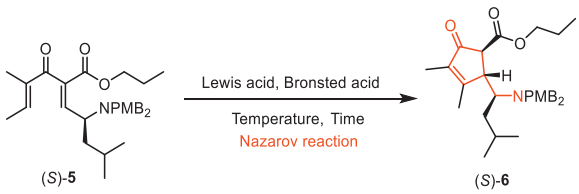

Entry	Lewis acid (equiv.)	Bronsted acid (equiv.)	Solvent	Temp (°C)	Time (h)	Yield (%)[b]
1	$SnCl_4$ (5)	No	DCE	25	8	25
2	$MeSO_3H$ (5)	No	DCM	25	8	ND
3	HCl (10)	No	1,4-Dioxane	25	8	ND
4	$Cu(OTf)_2$ (2)	No	DCM	25	8	ND
5	$Sc(OTf)_3$ (2)	No	DCE	25	8	trace
6	No	DPP (4)	DCE	25	8	ND
7	$In(OTf)_3$ (2)	DPP (4)	DCE	25	5	37
8	$Fe(OTf)_3$ (2)	DPP (4)	DCE	25	5	54
9	$Sc(OTf)_3$ (2)	DPP (4)	DCE	25	5	80
10	$Sc(OTf)_3$ (2)	DPP (4)	DCE	0	20	65
11	$Sc(OTf)_3$ (2)	DPP (2)	DCE	25	20	61
12	$Sc(OTf)_3$ (1)	DPP (2)	DCE	25	20	trace

[a] Reaction conditions: (*S*)–**5** (1.0 equiv.), 0.1 mol/L, air.
[b] Isolated yields.

When we extended previous reaction conditions with stoichiometric Lewis acids or protonic acids to our cyclization reaction, we rarely, if ever, obtained the corresponding cyclopentenone derivative (Table 1, entries 2–5). To our delight, the addition of stoichiometric Brønsted acid diphenyl phosphate (DPP) [46] allowed us to obtain the cyclopentenone product. Furthermore, the resulting cyclopentenone (*S*)–**6** with three contiguous stereocenters was obtained as a single enantiomer. However, Brønsted acid DPP alone was virtually inactive for the reaction (Table 1, entry 6). Among the metal salts tested, the scandium salt was found to be the most effective (Table 1, entries 7–9). The efficiency of the reaction was lower when the reaction temperature was reduced to 0 °C (Table 1, entry 10). By varying the amounts of $Sc(OTf)_3$ and DPP, we found that the optimal conditions were achieved with 2 equiv. of $Sc(OTf)_3$ and 4 equiv. of DPP. We speculate that the stoichiometric requirement of both Lewis and Brønsted acids may be attributed to the influence of the basic nitrogen. After many attempts, the optimal conditions (Table 1, entry 9) were identified, facilitating the production of cyclopentenone (*S*)–**6** as a single enantiomer in 80% yield from grams of (*S*)–**5**.

Conjugated addition of cyclopentenone (*S*)–**6** to an alkynone to form a *E*/*Z* mixture of **7** (*E*/*Z* 4.17:1). This was followed by oxidative debenzylation [47], and amine transesterification in one pot, generating 5/5 cyclopenta[*c*]pyrrol-one bicyclic **8** as a single *E* isomer. We speculate that the exclusive formation of one product is due to the lower energy of the *E*-form of compound **8** compared to the *Z*-form (see Supporting information for complete details). A reduction system of $CeCl_3{\cdot}7H_2O/NaBH_4$ reduced two carbonyl groups in compound **8**. Subsequently, one of the alcohols with less hindrance was selectively oxidized using MnO_2, yielding compound **2**, which is the C-7 hydroxyl stereoisomer of asperfilasin A. Compound **2** was conveniently transformed into asperfilasin A using Mitsunobu reaction in one pot. At the same time, a single crystal of **1** was obtained, allowing unambiguous determination of the absolute configuration of natural asperfilasin A.

It has been widely reported that cytochalasans exhibit cytotoxicity by targeting the actin cytoskeleton and affecting cellular processes such as cell adhesion, motility, signaling and cell division. Asperfilasin A was evaluated for its cytotoxic activities against seven cancer cell lines (HL60, NB4, Jurkat, MDA-MB-231, HEP-3B, HT29, and RKO). **1** exhibited more obvious cytotoxic effects against leukemia cell lines than other cells. The IC_{50} values of **1** against HL60 and NB4 cells were then obtained at a series of concentrations (14.1 ± 1.8 and 12.9 ± 3.9 μmol/L, respectively, Fig. S9g in Supporting information). Considering the best-known relaxation effect of cytochalasans, a confocal microscope fluorescence analysis with F-Actin was performed on HT29 cells treated with **1**, which suggested that **1** is an effective cytoskeletal inhibitor because F-actin was found to be disrupted relative to the control (Fig. S9c in Supporting information).

Then, compound **1** was tested to determine its influence on the cell cycle, which was found to cause G_2/M cycle arrest of HT29 cells (Figs. S9a and b in Supporting information). In a further study, **1** was observed to induce apoptosis of leukemia cells, with apoptosis assays performed on HL60 and NB4 cells *via* flow cytometry analyses. The results, in addition to the western bolt analyses on apoptosis-related proteins, indicated that **1** induced apoptosis of HL60 and NB4 cells by activation of caspase-3 and degradation of PARP (Figs. S9d-f in Supporting information). To better understand the mechanism by which compound **1** disrupted the cytoskeleton and induced cell cycle arrest, the binding modes of **1** with the crystal structure of monomeric actin were obtained by

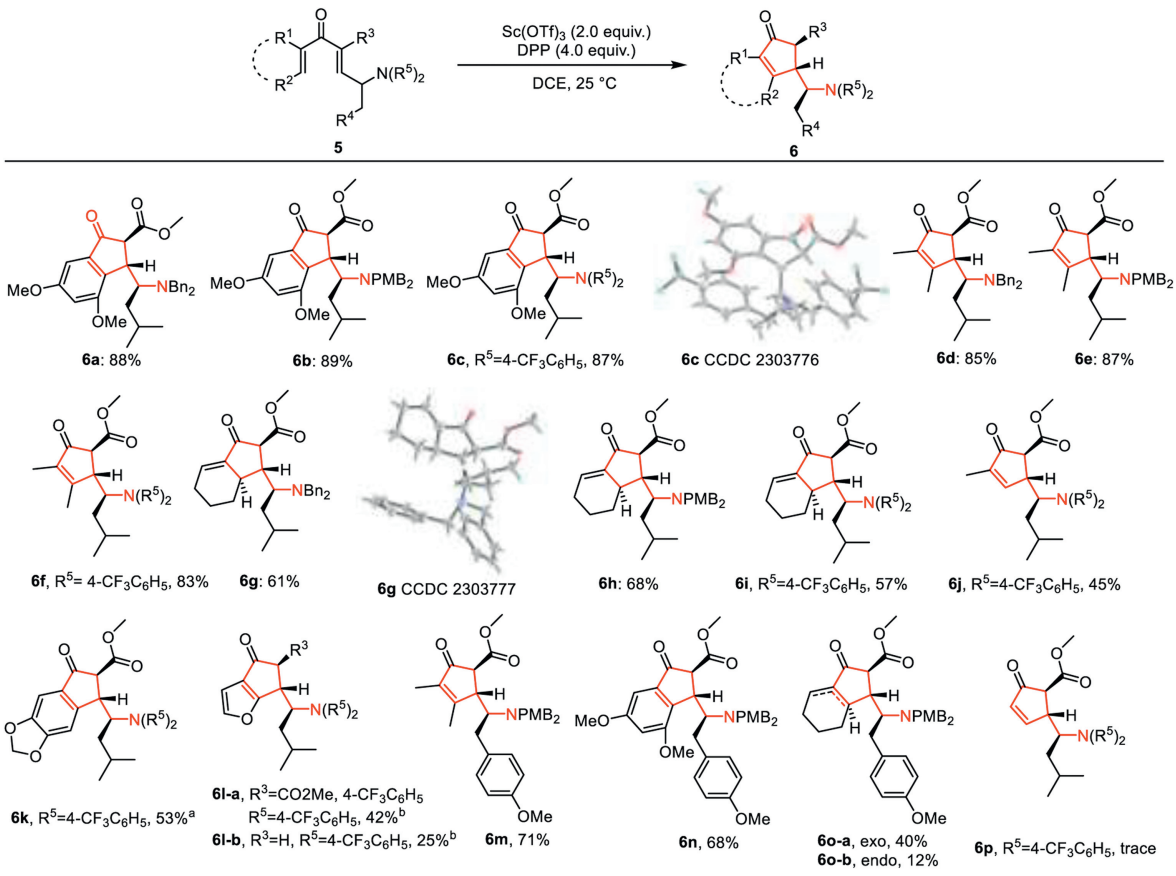

Scheme 4. Scope of substrate for the diastereoselective synthesis of cyclopentenones **6**. Standard conditions: $Sc(OTf)_3$ (2 equiv.), DPP (4 equiv.), 0.1 mol/L, 25 °C, air. Isolated yields. >20:1 *dr* values were observed for all of the products. [a] Condition: $Sc(OTf)_3$ (3 equiv.), DPP (6 equiv.). [b] Condition: $Sc(OTf)_3$ (4 equiv.), DPP (8 equiv.).

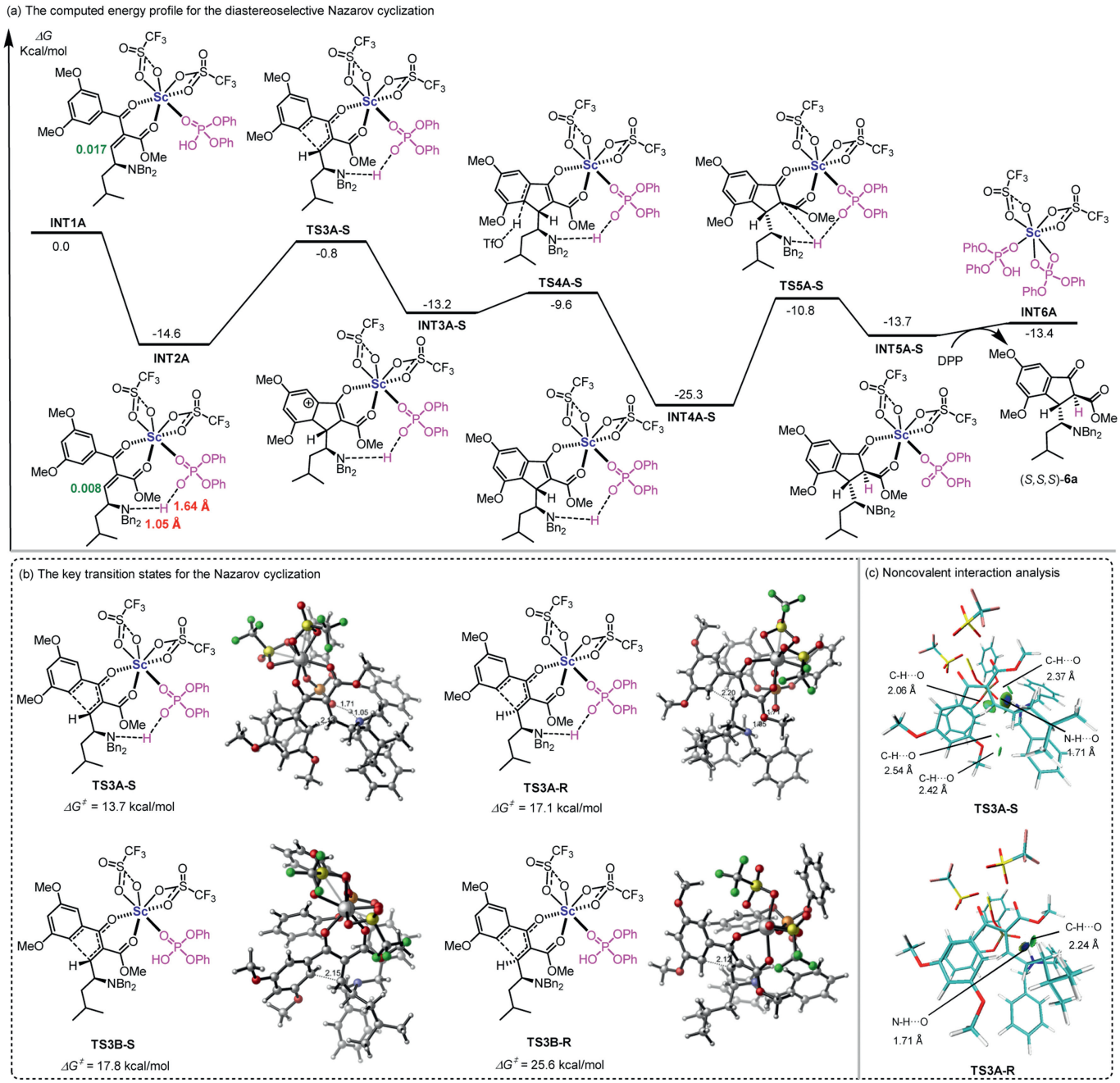

Fig. 1. DFT calculations for the Nazarov cyclization (DFT calculations were performed at the B3LYP-D3/6–311+G(d,p)-SDD/SMD (CH_2Cl_2)// B3LYP-D3/6–31G(d)-LANL2DZ level of theory).

molecular docking [48]. As shown in Fig. S9h (Supporting information), compound **1** could form hydrogen bonding interactions with residues Ile136, Gly168 and Ala170 and hydrophobic interactions with Tyr133, Ala135, Tyr169, Leu346 and Phe352. The calculated results predicted that compound **1** exhibited good binding affinity with monomeric actin.

During the total synthesis of **1**, the Nazarov cyclization containing basic nitrogen showed single regioselectivity and excellent diastereoselectivity. Having established the optimal reaction condition for the Nazarov cyclization above, the scope of the reaction was then investigated (Scheme 4). We noticed that this Nazarov reaction exhibited highly diastereoselective (dr > 20:1), even with three chiral centres in each case (**6a**-**6o**). Moreover, even products with four chiral centres were also formed (**6g**-**6i**, and **6o-a**). The reaction yields varied when the substituents on the benzene ring of the protecting groups were altered, with slightly higher yields observed for the electron-donating –OCH_3 group compared to the electron-withdrawing -CF_3 group. The electron-rich R^1 group was more favorable for Nazarov cyclization (**6c** and **6k**). Ring-closing reactions were more likely to occur when both R^1 and R^2 were highly substituted with methyl groups (**6f**, **6j** and **6p**). When the R^4 position was replaced by *p*-methoxyphenyl for isopropyl, only one diastereomer could be obtained as well. Compound **5l** yielded both the cyclopentenone product **6l-a** and the decarboxylation product **6l-b**, likely attributed to the increased stoichiometric amounts of $Sc(OTf)_3$ and DPP employed in the reaction [49,50]. Moreover, under the standard condition, compound **5o** not only produced the regular product **6o-a**, featuring a double bond outside the ring but also generated isomeric compound **6o-b**, characterized by a double bond inside the ring. We speculate that the larger R^4 group of **5o**

induces greater steric hindrance, influencing the regioselectivity of the reaction. The assigned structures were supported by the X-ray structures of compounds **6c** and **6g**.

To gain more insight into the reaction mechanism and the origin of the diastereoselectivity, density functional theory (DFT) calculations were performed on the Sc-mediated Nazarov cyclization of **5a** (Scheme 4). The initial ligand exchange leads to the formation of high equilibrium cationic intermediate **INT1A** bearing Sc catalyst, Brønsted acid DPP and substrate **5a** (Sc/DPP/**5a** = 1/1/1) [51-53]. Configurational isomerism of **INT1A** generates intermediate **INT2A**, in which the distances of O–H bond and N–H bond are 1.64 and 1.05 Å, respectively, indicating the existence of hydrogen bond between N atom in substrate and OH of DPP. The nature population analysis (NPA) charge distribution suggests the atomic charge of C_β in **INT1A** (0.017e) is more positive than that in **INT2A** (0.008e), revealing the formation of hydrogen increases nucleophilicity of C_β in **INT2A**, which renders the next conrotatory 4π electrocyclization easier. The detailed computational results also support this conclusion. Without the hydrogen bond interaction, the Nazarov cyclization through transition states **TS3B-S** and **TS3B-R** are calculated to have energy barriers of 17.8 and 25.6 kcal/mol, respectively, which are much higher than the same process through **TS3A-S** and **TS3A-R** (17.8 *vs.* 13.7 and 25.6 *vs.* 17.1 kcal/mol), indicating the importance of the hydrogen bond. For substrate **5a** with *S*-configuration, the formation of **INT3A-S** containing an *S*-intrinsic chirality and an *S*-induced chirality *via* transition state **TS3A-S** is kinetically more favorable (13.7 *vs.* 17.1 kcal/mol). The Nazarov cyclization is the diastereoselectivity-determining step and the origin of the induced enantioselectivity can be elaborated by the independent gradient model based on Hirshfeld partition (IGMH) (Fig. 1c) [54]. In the favored transition state **TS3A-S**, the *ortho* C–H bond of the phenyl group in the substrate forms a distinctive strong C–H···O interaction with the oxygen in DPP. This interaction significantly enhances the electron-rich characteristics of the *ortho* C–H bond, rendering it more vulnerable to nucleophilic attack and facilitating cyclization, thus reducing the energy barrier of **TS3A-S**. By comparison, the direct cyclization through transition **TS3A-R** is kinetically unfavorable due to the absence of significant non-covalent interactions. Subsequently, the following deprotonation of **INT3A-S** provides a thermodynamic driving force through the regeneration of aromaticity. The intermediate **INT4A-S** undergoes 1,4-hydrogen migration through transition state **TS5A-S** with an activation energy of 14.5 kcal/mol. Finally, the ligand exchange with another DPP releases the desired product (*S,S,S*)–**6a**. The computed results are consistent with the experimental observation, namely the diastereoselective formation of (*S,S,S*)–**6a** and (*R,R,R*)–**6a** when racemic **5a** was used as substrate.

Subsequently, several control experiments were conducted to gain insight into the mechanism of this reaction (Fig. S10 in Supporting information). The reaction of the deuterated substrate ***5a-D*** was carried out under standard conditions yielding 81% of the desired product. Subsequently, kinetic isotope control experiments (KIE) were performed. The results showed it is a secondary isotope effect in the experiments ($k_H/k_D = 0.89$), which suggested that the carbon atom linked to the isotope underwent a change in hybridization from sp^2 to sp^3, without bond cleavage occurring during the reaction process. The ring closing is the rate-determining step, consistent with DFT calculations.

In conclusion, asperfilasin A (**1**), with a unique 5/5 cyclopenta[*c*]pyrrol-one bicyclic core was discovered and characterized as the first example of cytochalasans that has 5/5 skeleton from *Aspergillus flavipes*. Moreover, asymmetric total syntheses of compound **1** was achieved in 7 steps from the easily prepared compound **4**, which not only corroborated the structural assignments for the compound but also provided a sufficient quantity of samples for further biological study. In the total synthesis studies of asperfilasin A, we developed a new Nazarov reaction containing basic nitrogen. A wide range of pentadienone substrates containing basic nitrogen were cyclized in excellent regioselective and diastereoselective manner. DFT calculations pinpoint that hydrogen bonding of cationic scandium(III) complexes to nitrogen atoms alters substrate torque selectivity, thereby affecting the diastereoselectively producing products. The bioassays revealed that **1** has obvious cytotoxic effects against leukemia cell lines. These findings suggest that **1** has potential as a promising lead compound for further pharmaceutical development.

Declaration of competing interest

The authors declare that they have no known competing financial interests or personal relationships that could have appeared to influence the work reported in this paper.

CRediT authorship contribution statement

Fengqing Wang: Writing – original draft, Validation, Investigation, Data curation, Conceptualization. **Changxing Qi:** Validation, Project administration. **Chunmei Chen:** Project administration, Investigation. **Qin Li:** Writing – original draft, Investigation. **Qingyi Tong:** Resources. **Weiguang Sun:** Resources. **Zhengxi Hu:** Validation. **Minyan Wang:** Writing – original draft, Software, Funding acquisition, Data curation. **Hucheng Zhu:** Writing – original draft, Project administration. **Lianghu Gu:** Supervision, Resources, Funding acquisition, Conceptualization. **Yonghui Zhang:** Writing – review & editing, Supervision, Resources, Funding acquisition.

Acknowledgments

This work was financially supported by the National Natural Science Foundation of China (Nos. 81725021, 81903461), the National Key R&D Program of China (No. 2022YFA1503200), the Natural Science Foundation of Hubei Province (No. ZRMS2023000340). We are extremely grateful to the High-Performance Computing Center of Nanjing University for doing the numerical calculations in this paper on its blade cluster system. We would like to thank Prof. Sheng Xiong Huang and Dr. Ming Yu (Kunming Institute of Botany, Chinese Academy of Sciences) for helpful advice about the biosynthetic pathways. We thank Prof. Youwei Xie, Prof. Junjun Liu and Suitian Lai for their helpful discussion and the Medical Subcenter of HUST Analytical & Testing Center for data acquisition. We are grateful to Prof. Chaomei Xiong, Prof. Zimin Lv and Mr. Wei Wang at the Tongji Medical College, Huazhong University of Science and Technology, for their help in the NMR spectrum and the mass spectrum.

Supplementary materials

Supplementary material associated with this article can be found, in the online version, at doi:10.1016/j.cclet.2024.110252.

References

[1] K. Scherlach, D. Boettger, N. Remme, et al., Nat. Prod. Rep. 27 (2010) 869–886.
[2] E. Skellam, Nat. Prod. Rep. 34 (2017) 1252–1263.
[3] D. Zhang, H. Ge, D. Xie, et al., Org. Lett. 15 (2013) 1674–1677.
[4] B.C. Yan, W.G. Wang, D.B. Hu, et al., Org. Lett. 18 (2016) 1108–1111.
[5] A. Berestetskiy, A. Dmitriev, G. Mitina, et al., Phytochemistry 69 (2008) 953–960.
[6] A. Cimmino, A. Andolfi, A. Berestetskiy, et al., J. Agric. Food Chem. 56 (2008) 6304–6309.
[7] A. Cimmino, M. Masi, M. Evidente, et al., Nat. Prod. Rep. 32 (2015) 1629–1653.
[8] H. Li, H. Wei, J. Hu, et al., ACS Chem. Biol. 15 (2020) 226–233.
[9] W. Gao, Y. He, F. Li, et al., Bioorg. Chem. 83 (2019) 98–104.
[10] Q.L. Mou, S.X. Yang, T. Xiang, et al., Tetrahedron Lett. 87 (2021) 153207.

[11] A. Makioka, M. Kumagai, S. Kobayashi, et al., Parasitol. Res. 93 (2004) 68–71.
[12] Y. Hu, W. Zhang, P. Zhang, et al., J. Agric. Food. Chem. 61 (2013) 41–46.
[13] H. Zhu, C. Chen, Q. Tong, et al., Progress in the chemistry of cytochalasans, in: A.D. Kinghorn, H. Falk, S. Gibbons, et al. (Eds.), Progress in the Chemistry of Organic Natural Products 114, Springer International Publishing, Cham, 2021, pp. 1–134.
[14] H. Zhu, C. Chen, Y. Xue, et al., Angew. Chem. Int. Ed. 54 (2015) 13374–13378.
[15] H. Zhu, C. Chen, Q. Tong, et al., Angew. Chem. Int. Ed. 55 (2016) 3486–3490.
[16] H. Zhu, C. Chen, Q. Tong, J, et al., Angew. Chem. Int. Ed. 56 (2017) 5242–5246.
[17] C. Tian, X. Lei, Y. Wang, et al., Angew. Chem. Int. Ed. 55 (2016) 6992–6996.
[18] M. Zaghouani, C. Kunz, L. Guédon, et al., Chem. Eur. J. 22 (2016) 15257–15260.
[19] X. Long, Y. Ding, J. Deng, Angew. Chem. Int. Ed. 57 (2018) 14221–14224.
[20] J.R. Reyes, N. Winter, L. Spessert, et al., Angew. Chem. Int. Ed. 57 (2018) 15587–15591.
[21] R. Bao, C. Tian, H. Zhang, et al., Angew. Chem. Int. Ed. 57 (2018) 14216–14220.
[22] X. Long, Y. Ding, H. Wu, et al., Synlett 31 (2020) 301–308.
[23] H. Wu, Y. Ding, K. Hu, et al., Angew. Chem. Int. Ed. 60 (2021) 15963–15971.
[24] J. Schümann, C. Hertweck, J. Am. Chem. Soc. 129 (2007) 9564–9565.
[25] T. Nakazawa, K.i. Ishiuchi, M. Sato, et al., J. Am. Chem. Soc. 135 (2013) 13446–13455.
[26] C. Wang, V. Hantke, R.J. Cox, et al., Org. Lett. 21 (2019) 4163–4167.
[27] C. Wang, K. Becker, S. Pfütze, et al., Org. Lett. 21 (2019) 8756–8760.
[28] J.M. Zhang, X. Liu, Q. Wei, et al., Nat. Commun. 13 (2022) 225.
[29] P.B. Knudsen, B. Hanna, S. Ohl, et al., Leukemia 28 (2014) 1289–1298.
[30] C. Chen, H. Zhu, J. Wang, et al., Eur. J. Org. Chem. 2015 (2015) 3086–3094.
[31] Z. Wang, S. Zhao, K. Zhang, et al., Synth. Syst. Biotechnol. 7 (2022) 1084–1094.
[32] J. Ouyang, J.L. Kennemur, C.K. De, et al., J. Am. Chem. Soc. 141 (2019) 3414–3418.
[33] Y. Que, H. Shao, H. He, et al., Angew. Chem. Int. Ed. 59 (2020) 7444–7449.
[34] Y. Zhang, Y. Chen, M. Song, et al., J. Am. Chem. Soc. 144 (2022) 16042–16051.
[35] F.T. Meng, X.Y. Qin, J. Li, et al., Chin. J. Chem. 40 (2022) 687–692.
[36] F.T. Meng, Y.N. Wang, X.Y. Qin, et al., Nat. Commun. 13 (2022) 7393.
[37] F.T. Meng, J.L. Chen, X.Y. Qin, et al., Org. Chem. Front. 9 (2022) 140–146.
[38] D.J. Kerr, J.M. White, B.L. Flynn, J. Org. Chem. 75 (2010) 7073–7084.
[39] D.J. Kerr, M. Miletic, J.H. Chaplin, et al., Org. Lett. 14 (2012) 1732–1735.
[40] N. Manchala, H.Y.L. Law, D.J. Kerr, et al., J. Org. Chem. 82 (2017) 6511–6527.
[41] R. Volpe, R.J. Lepage, Jonathan M. White, et al., Chem. Sci. 9 (2018) 4644–4649.
[42] B.L. Flynn, N. Manchala, E.H. Krenske, J. Am. Chem. Soc. 135 (2013) 9156–9163.
[43] E. Grenet, R. Robidas, A. van der Lee, et al., Eur. J. Org. Chem. 2022 (2022) e202200828.
[44] K.i. Ishiuchi, T. Nakazawa, F. Yagishita, et al., J. Am. Chem. Soc. 135 (2013) 7371–7377.
[45] D.J. Kerr, C. Metje, B.L. Flynn, Chem. Commun. (2003) 1380–1381.
[46] Z.G. Xi, L. Zhu, S. Luo, J.P. Cheng, J. Org. Chem. 78 (2013) 606–613.
[47] M. Yu, F. Wang, S. Yao, et al., Chin. J. Chem. 40 (2022) 2219–2225.
[48] U.B. Nair, P.B. Joel, Q. Wan, et al., J. mol. Biol. 384 (2008) 848–864.
[49] K. Komatsuki, Y. Sadamitsu, K. Sekine, K. Saito, T. Yamada, Angew. Chem. Int. Ed. 56 (2017) 11594–11598.
[50] H. Zhang, Z. Lu, Org. Chem. Front. 5 (2018) 1763–1767.
[51] T. Mietke, T. Cruchter, V.A. Larionov, et al., Adv. Synth. Catal. 360 (2018) 2093–2100.
[52] J.J. Koenig, T. Arndt, N. Gildemeister, et al., J. Org. Chem. 84 (2019) 7587–7605.
[53] Y.P. Chin, E.H. Krenske, J. Org. Chem. 87 (2022) 1710–1722.
[54] T. Lu, Q. Chen, J. Comput. Chem. 43 (2022) 539–555.